ISBN: 978-3-95450-191-5 doi:10.18429/JACoW-SRF2017-THPB005

DESIGN UPDATES ON CAVITY TO MEASURE SUPPRESSION OF MICROWAVE SURFACE RESISTANCE BY DC MAGNETIC FIELDS *

J. T. Maniscalco†, M. Liepe, and R. Porter
CLASSE, Cornell University, Ithaca, NY, 14853, USA

Abstract

Our research has shown good agreement between experimental measurements of the anti-Q-slope in niobium SRF cavities and predictions from a recent theoretical model of the suppression of the microwave surface resistance with applied RF field. To confirm that this mechanism is indeed what causes the anti-Q-slope in impurity-doped niobium, it will be necessary to measure the theory's prediction that the same effect may be achieved by applying a constant (i.e. DC) magnetic field parallel to the RF surface. This will also allow for systematic studies of the proposed fundamental effect of the anti-Q-slope and of the behavior of the anti-Q-slope for many surface preparations and alternative materials, since it provides a cleaner measurement by eliminating the counteracting quasiparticle overheating and the complexifying oscillation of the screening currents. In this report we give an update on work at Cornell to design and build a coaxial cavity to measure this effect.

MOTIVATION

The "anti-Q-slope" is a perplexing phenomenon, exhibited by certain impurity-doped niobium cavities, in which the microwave surface resistance decreases as the strength of the field in the cavity increases [1–3]. Soon after the discovery of this effect, theoretical work proposed a mechanism for this decrease in resistance: high magnetic fields establish Meissner-state screening currents on the superconducting surface, which modify the electron density of states in such a way that the surface resistance decreases [4]. However, as the RF field dissipates energy into the electrons in the surface, inefficiencies in the transfer of thermal energy out to the refrigeration system lead to an increasing electron temperature; this counterbalances the decrease in surface resistance due to the strong temperature-dependence of BCS theory [5, 6], and the magnitude of the anti-Q-slope can be tuned by the magnitude of the energy transfer inefficiency. Recent work from Cornell showed that the magnitude of this inefficiency depends linearly on the electron mean free path, the principal measure of doping strength for impurity-doped SRF cavities [7].

In order to confirm that this mechanism indeed is the source of the anti-Q-slope, it is necessary to measure another of the theory's predictions, namely that externally-applied constant (DC) magnetic fields parallel to the superconducting surface will also reduce the surface resistance. In this variation of the effect, the strong external DC field excites screening currents just as the RF field did in the above case. An experiment measuring this effect by measuring quality factor Q_0 with a low-power RF field (relative to the external DC field) would benefit from two simplifications compared with the original case: first, the weak RF field means that the oscillations in electron density with the RF field would not be significant in comparison to the changes due to the DC field; second, the weak RF field would dissipate only a small amount of power, leading to insignificant electron overheating. Because of these simplifications, in a sense such an experiment would be a "purer" investigation of the theory than experiments of the strong-RF case.

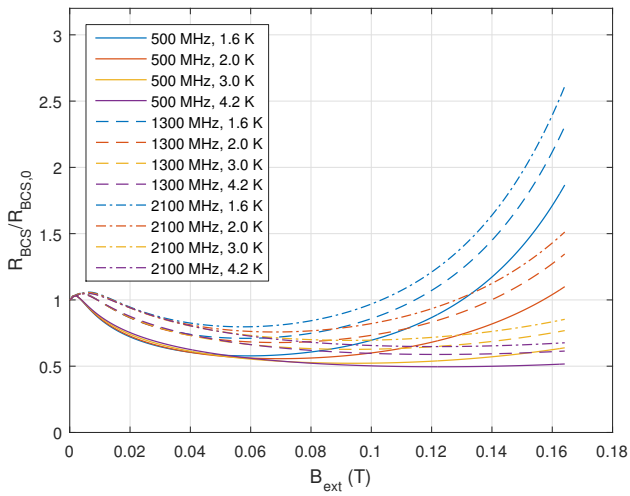

Figure 1: Theoretical predictions of the surface resistance (normalized to the zero-field value) for typical doped niobium parameters $\Delta/k_BT_c = 1.875$ and $\ell = 39$ nm.

Figure 1 shows theoretical predictions of the surface resistance as a function of DC field strength for several configurations of frequency and temperature. For magnetic fields up to ~ 50 mT, the greatest variation in the predictions of relative change in resistance depends on the RF frequency; for higher fields, on the other hand, the greatest variation in prediction comes from the dependence on temperature. To adequately investigate the theory experimentally, it will be necessary to probe both the frequency and temperature dependence of the effect.

The perfect diamagnetism of superconductors means that traditional cavities can not be used for such an experiment: superconducting cylinders are extremely efficient at shielding externally-applied magnetic fields [8]. As such, it is necessary to design a new cavity to perform these investiga-

* This work was supported in part by the U.S. National Science Foundation under Award No. PHY-1549132, the Center for Bright Beams, and under NSF Award No. PHY-1416318.
† jtm288@cornell.edu

ISBN: 978-3-95450-191-5 doi:10.18429/JACoW-SRF2017-THPB005

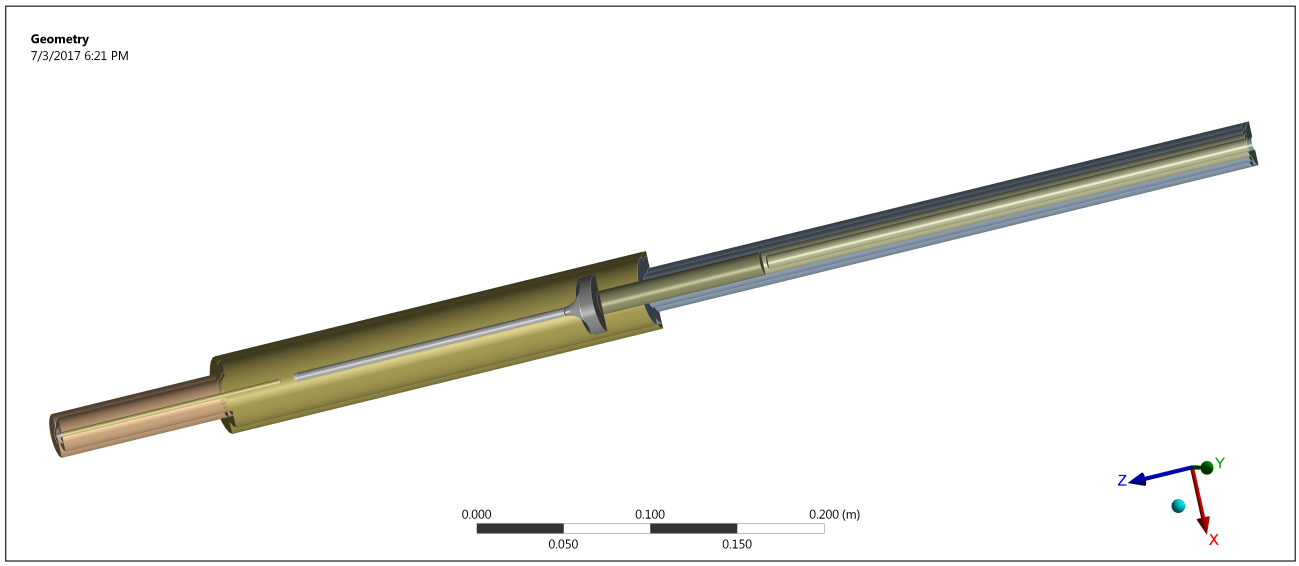

Figure 2: CAD representation of the coaxial cavity, from ANSYS. At left is the coupler, in the center is the resonator, and at right is the "thermal pathway" and enclosing tube.

tions. In this work we present one such design, in the form of a mixed-material coaxial resonator.

CAVITY DESIGN

The premise of our proposed experiment is to apply a strong external DC magnetic field onto a superconducting surface. To accomplish this, we chose a coaxial cavity design, with a superconducting inner conductor and normal-conducting outer conductor to allow the field from a magnet coil outside the cavity to penetrate to the RF surface. To investigate how the dependence of R_s on the RF field strength changes between different materials, the inner conductor is exchangeable, so that we may test many different surface treatments using the same cavity.

Because of the significantly higher surface resistance on the normal-conducting portion of the cavity, the "RF-Off" method of measuring the quality factor, commonly used in SRF R&D, cannot be used: the field decay would be dominated by the contribution from the outer conductor, so small changes to the surface resistance of the superconducting portion would be very small compared to the total surface resistance.

Instead, we chose a fundamentally different approach to measuring the surface resistance: the inner conductor is thermally isolated from the outer conductor, and measurements of the thermal gradient along the isolation pathway reveal the magnitude of the power dissipated on the inner conductor. Mathematically, the relation between the thermal gradient and the dissipated power is given by Eq. (1):

$$P = \Delta T \, \frac{\kappa A}{L} \tag{1}$$

Here, P is the dissipated power traveling down the thermal pathway, ΔT is the thermal gradient measured over a distance L along the pathway, κ is the thermal conductivity of the pathway, and A is the pathway's cross-sectional area.

For an SRF surface, the dissipated power is given by the surface integral in Eq. (2):

$$P(B_{DC}) = \frac{1}{2} \int |H_{RF}^2(s)| R_s(s, B_{DC}) \, ds \tag{2}$$

Here, $H_{RF}(s)$ is the local magnetic field magnitude and $R_s(s)$ is the local surface resistance at a point s on the surface.

In order to ensure that the dissipated power measured comes exclusively from the inner conductor, it is necessary to protect the thermal pathway from exposure to the RF field without thermally shorting to the outer conductor. Further, any instrumentation to measure the thermal gradient must also be protected from the RF field to prevent spurious measurements. To solve these problems, we chose a two-step thermal pathway.

First, a solid sapphire rod extends from the inner conductor into a tube with a smaller radius than the outer conductor. This portion of the cavity forms a circular waveguide with cutoff frequency higher than the experimental frequencies; as such there is very efficient field attenuation down the length of this section. Sapphire was chosen due to its very low loss tangent [9], which ensures low RF losses, as well as its low thermal conductivity [10, 11] which allows for high sensitivity in the thermal measurements (higher thermal gradient per unit power dissipated). The end of the inner conductor is flared outwards to protect the sapphire rod from high RF fields as well as to trap quarter-wave modes in the resonating portion of the cavity.

Second, the sapphire rod is connected on its other side to a capped hollow cylinder, made of niobium, running through the narrow outer cylinder out to the end of the cavity, where the two cylinders are joined, thermally connecting the inner conductor to the liquid helium bath outside the cavity.

ISBN: 978-3-95450-191-5 doi:10.18429/JACoW-SRF2017-THPB005

The interior of this cylinder will also be kept at vacuum, with temperature sensors placed at several locations spaced along its length to measure the temperature gradient over the thermal pathway.

Figure 2 shows the completed RF design of the cavity, in longitudinal cross-section. Its overall dimensions are a length of 73 cm and an outer radius of 2.3 cm. The inner conductor has a length of 19 cm, with a radius of 0.25 cm on the narrow rod and 1.7 cm on the wider flared part; the very narrow radius ensures high power dissipation and thus high sensitivity to changes in surface resistance due to the applied field. The sapphire rod has a radius of 0.7 cm and a length of 10 cm; the niobium cylinder has an outer radius of 0.7 cm, an inner radius of 0.4 cm, and a length of 30 cm.

With the given dimensions and an estimated thermal conductivity of 10 W/Km for niobium [12], this design yields a thermal gradient along the niobium cylinder of 290 mK per mW dissipated on the inner conductor.

RF SPECIFICATIONS

As mentioned above, the main resonant mode of this cavity closely resembles the quarter-wave mode, with peak electric field at the rounded tip of the inner conductor and peak magnetic field at the narrow portion closest to the flared region of the inner conductor. Figure 3 shows this mode, at ≈ 500 MHz, as well as two higher modes at 1300 MHz and 2100 MHz; these higher modes allow investigation of the frequency-dependence of this effect. For the fundamental mode, the ratio of peak electric to peak magnetic field strengths is 0.67 MV/m/mT; calculations for the second and third modes yield similar results. Scaled to a total power dissipation of 16 W (dominated by a copper outer conductor), the peak electric and magnetic field strengths of the fundamental mode are 12 MV/m and 18 mT. RF losses on the inner conductor account for approximately 5×10^{-5} W per W dissipated in the entire cavity. Losses on the sapphire rod and the hollow niobium cylinder are negligible.

The coupler, which will be movable in the physical implementation of the cavity, is a simple rod antenna that extends through a coupler port into the resonating region of the cavity, coupling to the electric field, similar to the couplers used at Cornell for single-cell TESLA cavity tests. We performed RF simulations to ensure that the range of motion of the coupler allows for a coupling constant β from 0.1 to 1 for each of the modes, assuming a range of travel of 4 cm.

ENGINEERING SIMULATIONS

We performed several simulations to ensure that the cavity is mechanically sound. The main point of concern is the narrow central rod of the design: isolating the inner conductor thermally has the downside of limiting mechanical stability. In particular, the electromagnet surrounding the cavity will generate forces on the inner conductor (due to the flux-expelling surface currents), squeezing radially inwards on the thin rod portion and pushing the flared portion upwards towards the tube portion. Under an external field of

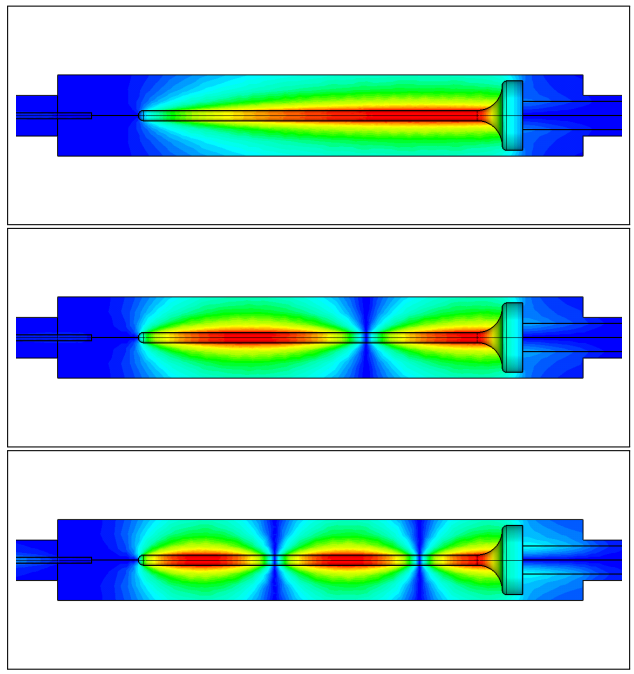

Figure 3: Magnetic fields of the first three RF modes in the cavity, at 500 MHz, 1300 MHz, and 2100 MHz. Images generated in CST studio.

100 mT, we found that this upward force was of magnitude 1 N; mechanical calculations in ANSYS showed that this force was well below the buckling threshold (with a safety factor of ≈ 2000).

We performed further mechanical simulations of air pressure (with vacuum inside the cavity) and of gravity (with the cavity lain on its side), with similarly safe results. We also studied random mechanical vibration; though we do not know of a sufficient vibration spectrum for the Cornell SRF test facilities, we employed the MIL-STD-810G spec for highway cargo as what we believe to be a significant overestimate of vibration magnitude, and found 2σ vibrations of 30 µm or lower for the entire cavity. As a result, we expect that random vibrations will not cause significant detuning issues. Lorentz force simulations yielded similarly small vibrations.

MAGNET DESIGN

As mentioned previously, the DC magnetic field will be generated by an electromagnet coil oriented coaxially outside the cavity. Because of the sensitivity of the field dependence of the suppression of the surface resistance, a standard solenoid will not be sufficient in terms of field uniformity. Instead, it is necessary to design a magnet with very uniform field along the axis. In order to accomplish this, we have used a genetic algorithm to design a coil winding pattern to produce a field that is flat within tolerance.

The design of this winding pattern is not yet finalized, but Fig. 4 shows one potential winding pattern generated

ISBN: 978-3-95450-191-5 doi:10.18429/JACoW-SRF2017-THPB005

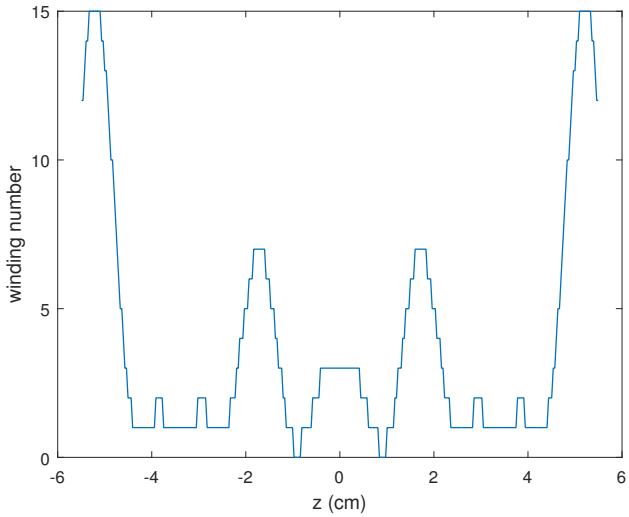

Figure 4: One possible winding pattern to yield a highly uniform magnetic field, generated by a genetic algorithm. Y-axis values indicate number of wire layers at each position.

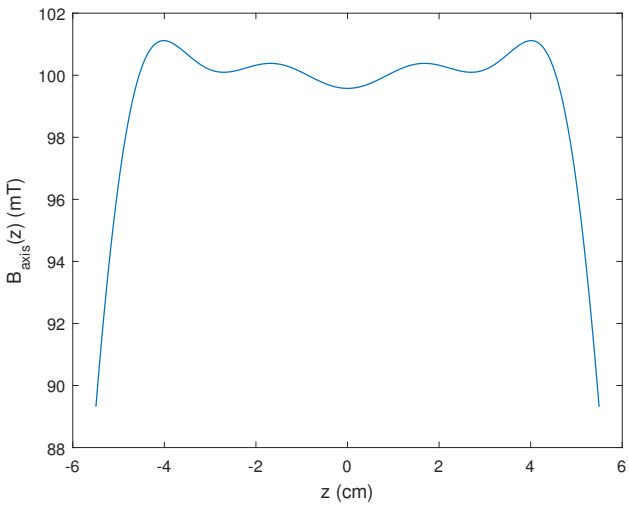

Figure 5: The axial magnetic field resulting from the winding pattern shown in Fig.4, set to a current of 10 A.

with the above method; Fig. 5 shows the resulting axial field, with very high uniformity.

Very soon at Cornell we will be constructing prototype magnets to verify our design method. In the final implementation, the magnet will be wound with NbTi superconducting wire.

Finally, to protect the test equipment such as the cryogenic dewar and cavity insert assembly from the high magnetic fields generated by the electromagnet, the resonator portion of the cavity (magnet included) will be surrounded by a superconducting magnetic shield. Figure 6 shows the mechanical design of the magnet and shielding as well as the effectiveness of the shielding even in the case where there are 1 mm cracks between the cylindrical portion and the end caps; in the second image, red areas indicate fields above 100 μT (1 G) when the magnet is set to 100 mT.

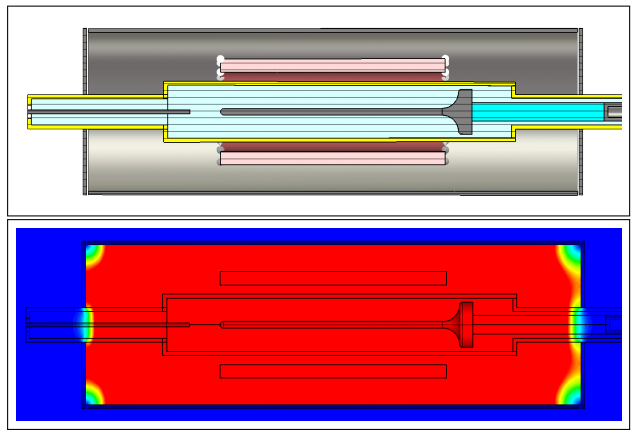

Figure 6: Above is the mechanical design of the magnet and shielding around the resonator; below is the DC field profile, indicating the effectiveness of the superconducting shielding. Red areas indicate fields higher than 0.1% of the electromagnet's peak field strength.

NEXT STEPS

The design for this cavity is nearly complete. The immediate next steps are to build a prototype magnet and test for field uniformity to verify our genetic algorithm method. Following this, we will finalize the mechanical design of the cavity, finalize the winding pattern design, build and test the full electromagnet, and finally build the cavity. The simple cylindrical shapes in the cavity (aside from the inner conductor's flared edge) should make fabrication simple and rapid.

CONCLUSION

We have made significant progress in the design and simulation of a coaxial SRF resonator to test the recent theoretical prediction of the suppression of the surface resistance by externally applied constant (DC) magnetic field. Testing this phenomenon requires several unique features, including a thermally-isolated inner conductor and a highly uniform external field; we believe that our design achieves these goals. We have performed numerous simulations of both the mechanical and electromagnetic performance of the cavity, with satisfying results. In the coming months we will proceed with prototype magnet development and testing, followed by finalization of the design and fabrication.

REFERENCES

[1] A. Grassellino, A. Romanenko, D. Sergatskov, O. Melnychuk, Y. Trenikhina, A. Crawford, A. Rowe, M. Wong, T. Khabiboulline, and F. Barkov, "Nitrogen and argon doping of niobium for superconducting radio frequency cavities: a pathway to highly efficient accelerating structures," *Superconductor Science and Technology*, vol. 26, no. 10, p. 102001, 2013. [Online]: http://stacks.iop.org/0953-2048/26/i=10/a=102001

[2] P. Dhakal, G. Ciovati, G. R. Myneni, K. E. Gray, N. Groll, P. Maheshwari, D. M. McRae, R. Pike, T. Proslier, F. Stevie,

ISBN: 978-3-95450-191-5 doi:10.18429/JACoW-SRF2017-THPB005

R. P. Walsh, Q. Yang, and J. Zasadzinzki, "Effect of high temperature heat treatments on the quality factor of a large-grain superconducting radio-frequency niobium cavity," *Phys. Rev. ST Accel. Beams*, vol. 16, p. 042001, Apr 2013. [Online]: http://link.aps.org/doi/10.1103/PhysRevSTAB.16.042001

[3] D. Gonnella, "The fundamental science of nitrogen-doping of niobium superconducting cavities," Ph.D. dissertation, Cornell University, 2016.

[4] A. Gurevich, "Reduction of dissipative nonlinear conductivity of superconductors by static and microwave magnetic fields," *Phys. Rev. Lett.*, vol. 113, p. 087001, Aug 2014. [Online]: https://link.aps.org/doi/10.1103/PhysRevLett.113.087001

[5] J. Bardeen, L. N. Cooper, and J. R. Schrieffer, "Microscopic theory of superconductivity," *Phys. Rev.*, vol. 106, pp. 162–164, Apr 1957. [Online]: http://link.aps.org/doi/10.1103/PhysRev.106.162

[6] J. Bardeen, L. N. Cooper, and J. R. Schrieffer, "Theory of superconductivity," *Phys. Rev.*, vol. 108, pp. 1175–1204, Dec 1957. [Online]: http://link.aps.org/doi/10.1103/PhysRev.108.1175

[7] J. T. Maniscalco, D. Gonnella, and M. Liepe, "The importance of the electron mean free path for superconducting radio-frequency cavities," *Journal of Applied Physics*, vol. 121, no. 4, p. 043910, 2017. [Online]: http://dx.doi.org/10.1063/1.4974909

[8] J. J. Rabbers, M. P. Oomen, E. Bassani, G. Ripamonti, and G. Giunchi, "Magnetic shielding capability of mgb 2 cylinders," *Superconductor Science and Technology*, vol. 23, no. 12, p. 125003, 2010. [Online]: http://stacks.iop.org/0953-2048/23/i=12/a=125003

[9] N. Pogue, P. McIntyre, A. Sattarov, and C. Reece, "A measurement device of the loss tangent and heat capacity of a large single crystal and the impact on the design of wafer sample cavity," in *Proceedings of SRF2011, Chicago, IL*, 2011.

[10] R. Berman, E. L. Foster, and J. M. Ziman, "Thermal conduction in artificial sapphire crystals at low temperatures. i. nearly perfect crystals," *Proceedings of the Royal Society of London A: Mathematical, Physical and Engineering Sciences*, vol. 231, no. 1184, pp. 130–144, 1955. [Online]: http://rspa.royalsocietypublishing.org/content/231/1184/130

[11] M. W. Wolfmeyer and J. R. Dillinger, "The thermal conductivity of sapphire between 0.4 and 4° K," *Physics Letters A*, vol. 34, pp. 247–248, Mar. 1971.

[12] S. M. Wasim and N. H. Zebouni, "Thermal conductivity of superconducting niobium," *Phys. Rev.*, vol. 187, pp. 539–548, Nov 1969. [Online]: https://link.aps.org/doi/10.1103/PhysRev.187.539